Lukáš Faturík
Libor Trško
Slavomír Hrček
Otakar Bokůvka

ISSN 1333-1124
eISSN 1849-1391

COMPARISON OF STRUCTURAL DESIGN IN HIGH AND ULTRA-HIGH CYCLE FATIGUE REGIONS

UDC 669.15:539.42

Summary

Ultra-high cycle fatigue of structural materials has been an extensively investigated phenomenon in the last thirty years. Nevertheless, the fact that there is no infinite fatigue life of metallic materials has not been considered in structural design very often. This paper presents the results of 50CrMo4 low alloy steel fatigue tests in the high and the ultra-high cycle region showing a considerable difference in the fatigue strength for $N = 10^7$ and $N = 10^9$ loading cycles. A comparison of shaft mechanical design for different required fatigue lifetimes is provided showing a necessity of designs changes to achieve safe operation in the ultra-high cycle region, thus leading to a 10 % increase in the weight of the shaft.

Key words: *50CrMo4 steel, ultra-high cycle fatigue, high frequency fatigue testing, mechanical design, shaft*

1. Introduction

The present development of new industrial machines which require higher efficiency and cost savings must provide a possibility of higher loadings, higher operating speeds and high reliability with fewer requirements for maintenance. For example, components of the high speed train Shinkanzen have to withstand approximately 10^9 cycles in 10 years of operation and failure of a main component can have fatal consequences [1]. These facts have imposed requirements for fatigue life testing in the so-called ultra-high cycle (UHC) region. Then, it must be assessed if the fatigue strength of a material could be really considered constant for more than 10 million cycles, which is the usual number of cycles used to determine the so-called fatigue limit. From the first tests performed by exceeding the number of cycles used for the determination of conventional fatigue limit it was obvious that fatigue failures can occur even at lower values of applied stress amplitudes than that of the fatigue limit, which means after a number of cycles much above 10^7 [2-5].

Except for special applications including aeronautical structures or jet engines, the decrease in fatigue strength after the conventional fatigue limit is not considered in ordinary structural applications. It is assumed that the decrease in the fatigue limit is compensated for by the safety coefficients which are used in mechanical design. However, due to the weight and the cost efficiency, there is a trend towards decreasing these safety coefficients as much as possible. Nowadays, a great number of common structural components often greatly

exceed the number of loading cycles used for standard fatigue limit evaluation ($N = 10^7$ cycles); ignoring the decrease in the fatigue strength after this number of cycles can create a great potential risk for the safe operation and reliability of a particular device [6].

This article presents an example of mechanical design of a shaft connecting gears in a gearbox manufactured from 50CrMo4 steel. The aim is to compare dimensions and parameters of the shaft when it is designed for the fatigue strengths evaluated for $N = 10^7$ cycles and $N = 10^9$ cycles.

2. Experimental material and fatigue tests

Quenched and tempered 50CrMo4 steel was considered in this study. The nominal chemical composition is shown in Table 1. The used steel was die forged in the temperature range 850 - 1050 °C. After forging, the material was quenched from the austenization temperature of 860 °C (holding time - 1 hour) in mineral oil. Right after quenching, the steel was tempered at the temperature of 600 °C for 1 hour and then it was left to cool in the still air. The heat treatment resulted in mechanical properties listed in Table 2.

Table 1 Chemical composition of 50CrMo4 steel according to DIN EN 10083-3 (wt. %)

C	Mn	Si (max.)	P (max.)	S (max.)	Cr	Mo	Fe
0.46 ÷ 0.54	0.50 ÷ 0.80	0.40	0.025	0.035	0.90 ÷ 1.2	0.15 ÷ 0.30	balance

Table 2 Mechanical properties of 50CrMo4 steel after quenching and tempering

UTS /MPa	Proof stress /MPa	A /%	Z /%
929	702	15.0	54.7

It is not possible to perform fatigue tests aimed at investigating the ultra-high cycle fatigue region by means of conventional low frequency fatigue testing methods because the duration of the test would be more than a year. Therefore, a special high frequency ultrasonic testing device based on the mechanical resonance of the ultrasonic system is used for this purpose to test the specimen (Fig. 1) at a frequency of $f \approx 20$ kHz [7]. During the test, the specimen is cooled in an aqueous solution of corrosion inhibitor to prevent the effect of the increased temperature of the experimental material on the measurement.

Results of high frequency tension - compression fatigue tests performed at a frequency of $f \approx 20$ kHz, temperature $T = 20 \pm 5$ °C, and cycle asymmetry ratio $R = -1$ show a decreasing character of the fatigue life curve (Fig. 2) at lower values of stress amplitudes than that of the conventional fatigue limit evaluated for $N = 10^7$ cycles. To obtain the mathematical dependence of the number of cycles to failure on the loading stress amplitudes, experimental results were approximated by the Basquin function, using the least square method [8]:

$$\sigma_a = \sigma'_f (N_f)^b \tag{1}$$

where b is the exponent of fatigue life curve and σ'_f is the coefficient of fatigue toughness obtained by the extrapolation of stress amplitude on the first loading cycle [9,10]. Regression curve coefficients are given in Table 3. When the increasing number of cycles is considered, a significant decrease in the fatigue strength is noted after the conventional fatigue limit for $N = 10^7$ cycles (Table 4). The difference between the fatigue limit for $N = 10^7$ cycles and for $N = 10^9$ cycles reaches a value of $\Delta\sigma_a = 151.5$ MPa.

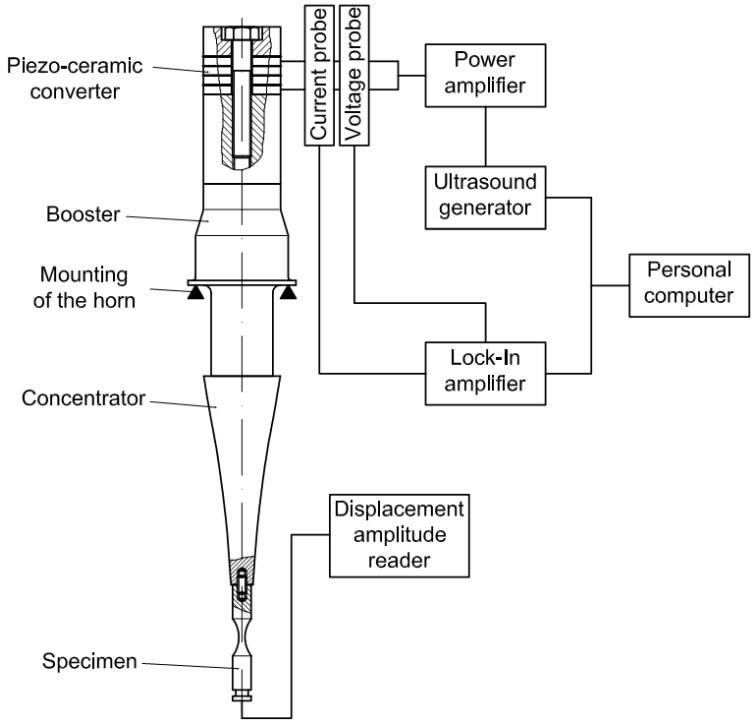

Fig. 1 Device for ultrasonic fatigue tests at frequency f ≈ 20 kHz

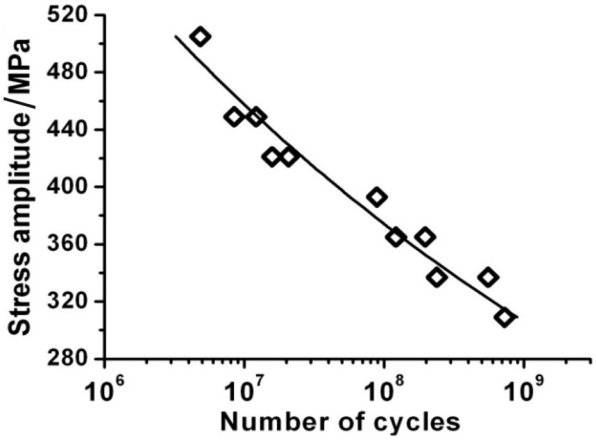

Fig. 2 S – N curve of 50CrMo4 steel

Table 3 Regression curve coefficients

Material	σ'_f /MPa	b
50CrMo4	1869	-0.0873

Table 4 Fatigue strength for different numbers of loading cycles according to regression curves

Fatigue strength for $N = 10^7$ /MPa	Fatigue strength for $N = 10^8$ /MPa	Fatigue strength for $N = 10^9$ /MPa
457.6	374.3	306.1

3. Mechanical design of a shaft for different fatigue limits

Examples of the differences in mechanical design of a shaft when different operational lifetimes are considered will be given for a gearbox shaft with frontal (Z_2) and conic (Z_3) gears (Fig. 3). The shaft is loaded by a torque moment M_{t2max} = 7500 N·m, which represents the highest loading value. However, the short-time overload of the shaft might be present at the machine start-up, but this loading is usually just in the area of low-cycle fatigue and that is why it is not considered in this example of the shaft design for the high and the ultra-high cycle fatigue.

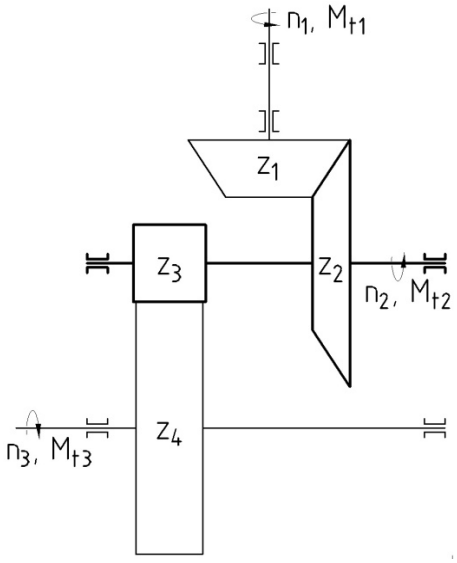

Fig. 3 Sketch of the gearbox; the analyzed shaft with gears is marked by darker lines

3.1 Verification of static safety of the shaft

Firstly, it is necessary to analyze the values of loading forces on the axial (2), radial (3) and tangential (circumferential) (4) components:

$$F_a = F_t \cdot \mathrm{tg}\,\alpha \cdot \cos\delta \tag{2}$$

$$F_r = F_t \cdot \mathrm{tg}\,\alpha \cdot \sin\delta \tag{3}$$

$$F_t = \frac{2 \cdot M_t}{d} \tag{4}$$

where F is the force (N), M_t is the torque moment (N·m), α is the pressure angle of the gear teeth (angle of obliquity) (20°), δ is the pitch-cone angle of the bevel gear (71.38°) and d is the mean value of the pitch diameter [11,12].

Results of the force components, graphically shown in Figure 4, are as follows:

Tangential forces:

$$F_{t12} = \frac{2 \cdot M_{t2\max}}{d_2} = \frac{2 \cdot 7\,500}{0.332} = 45\,181\ \mathrm{N} \tag{5}$$

$$F_{t43} = \frac{2 \cdot M_{t2\max}}{d_3} = \frac{2 \cdot 7\,500}{0.135} = 111111\ \mathrm{N} \tag{6}$$

Radial forces:

$$F_{r12} = F_{t12} \cdot \mathrm{tg}\,\alpha \cdot \sin\delta_2 = 45\,181 \cdot \mathrm{tg}\,20° \cdot \sin 71.38° = 15\,584\ \mathrm{N} \tag{7}$$

$$F_{r43} = F_{t43} \cdot \mathrm{tg}\,\alpha \cdot \sin\delta_2 = 111111 \cdot \mathrm{tg}\,20° \cdot \sin 71.38° = 40\,441\ \mathrm{N} \tag{8}$$

Axial forces:

$$F_{a12} = F_{t12} \cdot \mathrm{tg}\,\alpha \cdot \cos\delta_2 = 45\,181 \cdot \mathrm{tg}\,20° \cdot \cos 71.38° = 5\,251\ \mathrm{N} \tag{9}$$

$$F_{a43} = 0 \tag{10}$$

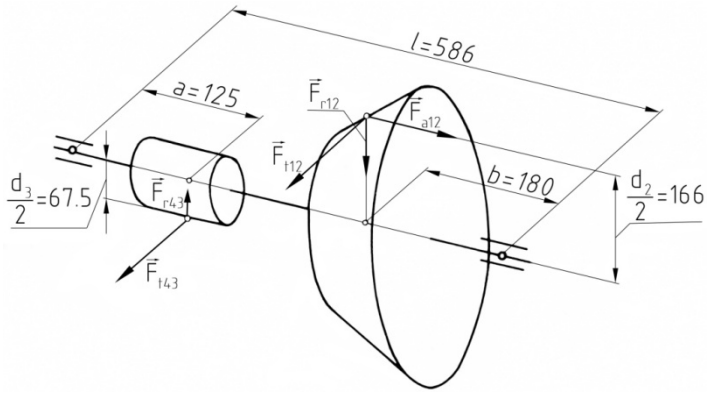

Fig. 4 Sketch for the analysis of the axial (F_a), radial (F_r) and tangential (F_t) components of the loading forces

Since the loading forces F_t, F_r and F_a are not oriented in the same plane, it is necessary to analyze the bending moments in two perpendicular planes, x-z and y-z (Fig. 5). The resulting bending moments are obtained by the vector sum of the partial bending moments (Fig. 6). To analyze the stress in the shaft, it is necessary to consider loadings in the points 1-6 (marked in Figs. 5 and 6). Table 5 shows the values of the bending stress (11), shear stress (12) and von Mises stress (13) which are obtained using the following equations:

$$\sigma_{bi} = \frac{M_{bi}}{W_{bi}} \tag{11}$$

$$\tau_{ki} = \frac{M_{ti}}{W_{ti}} \tag{12}$$

$$\sigma_{red} = \sqrt{\sigma_{bi}^2 + 3 \cdot \tau_{ti}^2} \tag{13}$$

where σ_{bi} is the bending stress (Pa), τ_{ki} is the shear stress (Pa), σ_{red} is the von Mises stress, M_b is the bending moment (N·m), W_b is the bending section modulus (m^3), M_t is the torque moment (N·m), W_t is the torque section modulus (m^3), and τ_t is the shear stress (Pa) [13,14].

Table 5 Resulting bending and torque moments in points 1 – 6

Point *i*	1	2	3	4	5	6
Bending moment M_{bi} /Nm	4 002.2	8 425.7	12643.1	9 905.3	5 502.9	2 091.1
Torque moment $M_{t2\text{-}i}$ /Nm	0	0	7500	7500	0	0

Point *i*	1	2	3	4	5	6
Bending stress σ_{bi} /MPa	55.9	100.1	74.5	95.1	65.4	29.2
Shear stress τ_{ti} /MPa	0	0	22.1	36	0	0
von Mises stress σ_{redi} /MPa	55.9	100.1	83.8	113.7	65.4	29.2

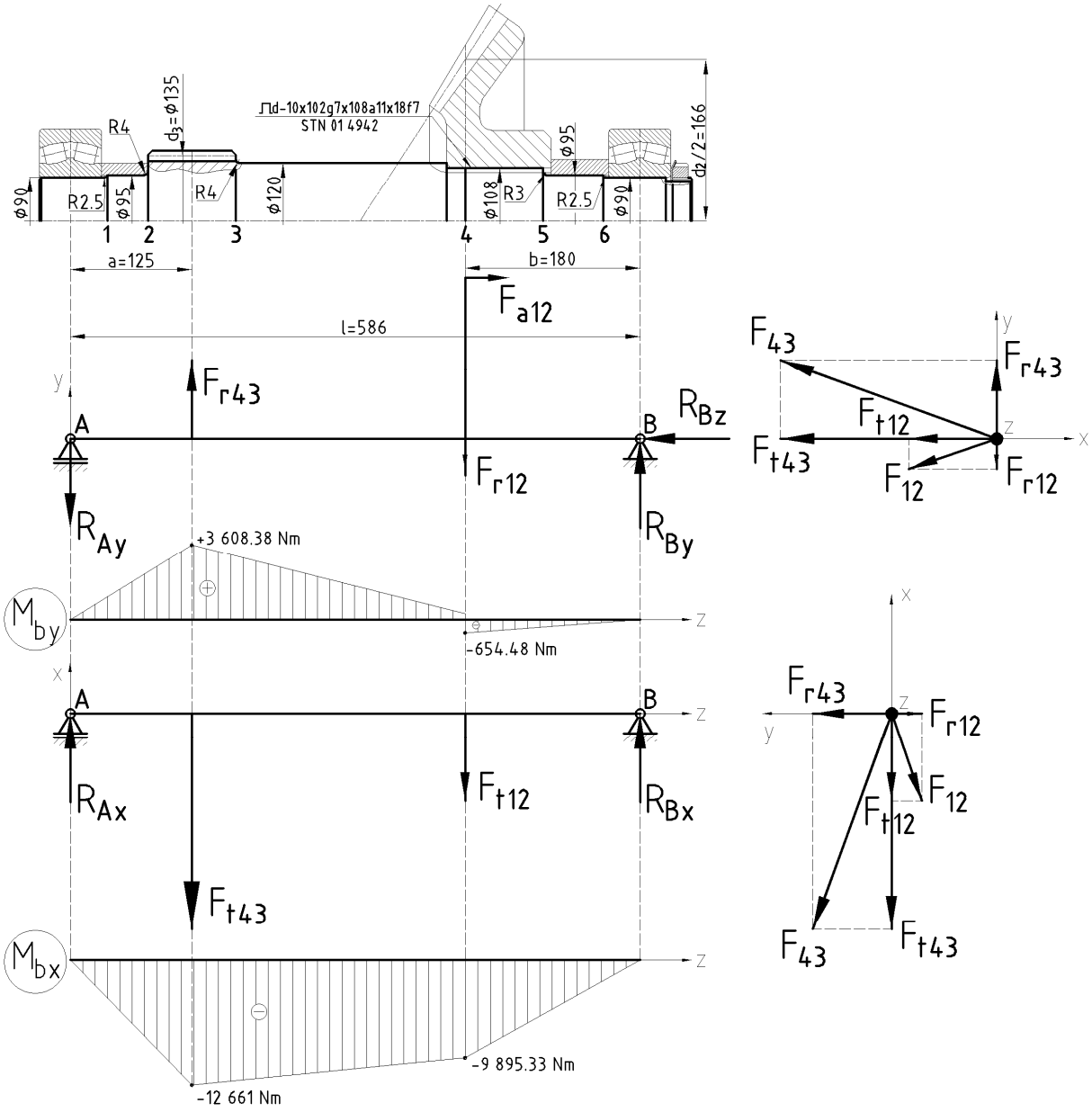

Fig. 5 Partial bending moments in two perpendicular planes x-z and y-z

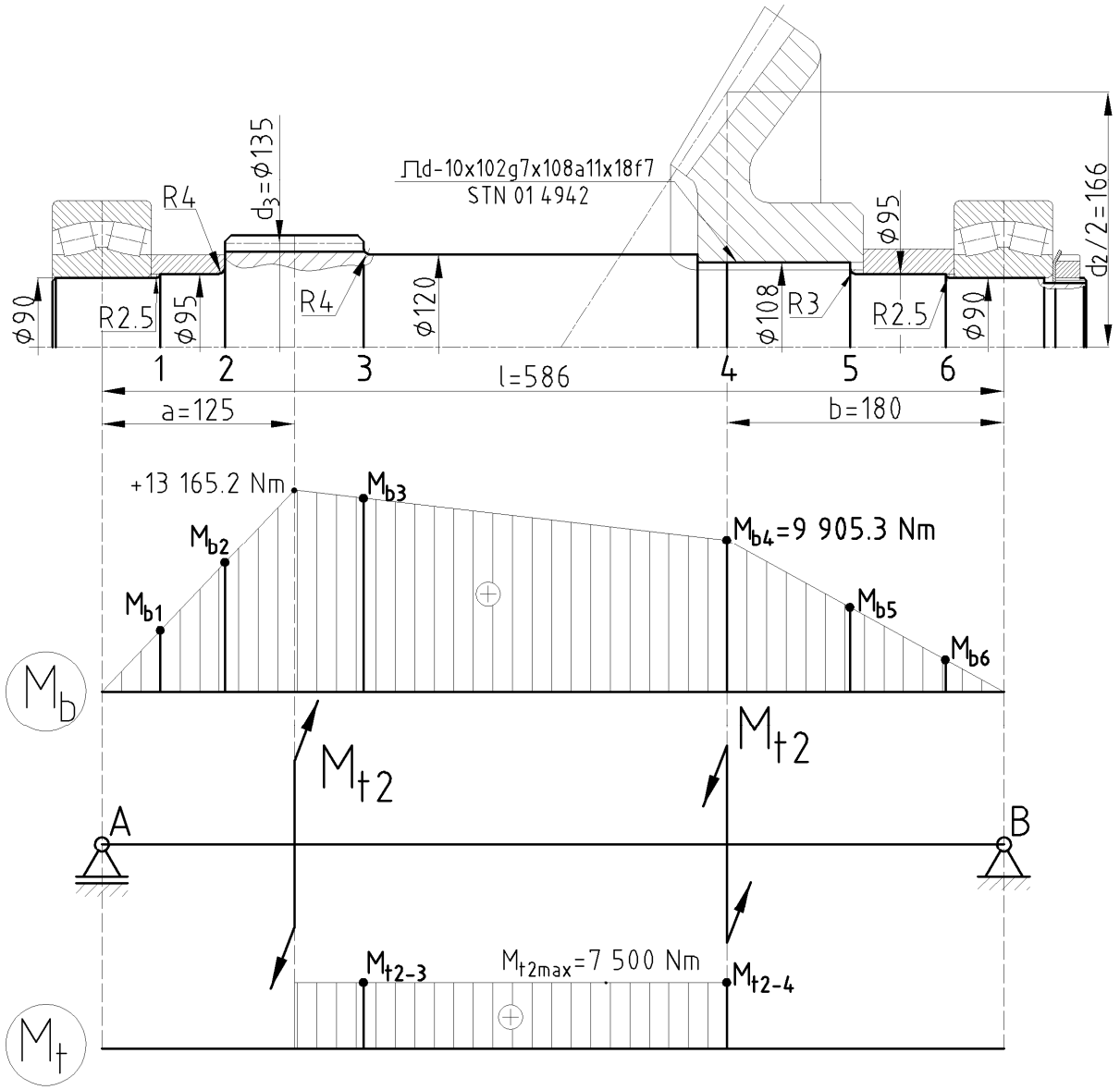

Fig. 6 Resulting bending and torque moments in the analyzed shaft

In Table 5 one can see that the highest value of von Mises stress (σ_{red}) is in the point 4 (Fig. 6), which means that this point is subjected to the highest load; therefore, this is a critical region of the shaft. The value of the static safety coefficient is evaluated according to equation (14):

$$k_s = \frac{R_{p0.2}}{\sigma_{red\,4}} = \frac{702}{113.7} = 6.17 \tag{14}$$

where k_s is the static safety coefficient, $R_{p0.2}$ is the proof stress (Pa) and $\sigma_{red\,4}$ is the von Mises stress in the point 4 (Pa). The value of the resulting static safety coefficient is very high, which results in high safety in terms of static loading and which assumes that the shaft is over equipped. However, a determining factor for safe operation is the cyclic loading; therefore, it is necessary to verify the shaft in terms of fatigue lifetime.

3.2 Verification of fatigue safety of the shaft

The shaft fatigue safety will be verified in the points 2 and 4 (Fig. 6) where the highest static loadings and also notches are present. The example of verification of point 4 is drawn in detail and the results for both verified points are given in Table 6. To compare the differences in the shaft size, the shaft safety will be verified with respect to the fatigue strength in the regions of high-cycle fatigue ($N = 10^7$ cycles) and of ultra-high-cycle fatigue ($N = 10^9$ cycles).

As the shaft is fitted into bearings so that it can turn, the forces created by meshing gears are not changing. Hence, it can be considered that the shaft is loaded by symmetrical bending cyclic loading, with a cycle asymmetry ratio of $R = -1$ (Fig. 7a). For the torsional fatigue loading, the discrete loading in operation is considered; therefore, the shaft will be loaded by a disappearing cycle, with a cycle asymmetry ratio of $R = 0$ (Fig. 7b).

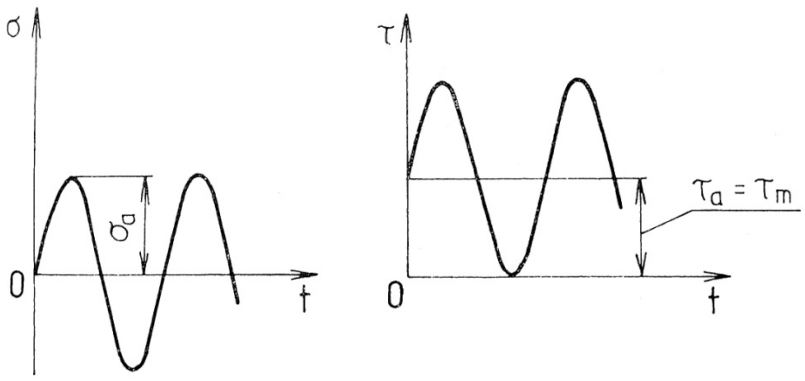

Fig. 7 Types of shaft fatigue loading: bending loading (a) and torque loading (b)

Bending loading (point 4)

Fatigue limit of 50CrMo4 steel for $N = 10^7$ cycles, tested on small (diameter of 4 mm), polished (Ra = 0.4 μm) specimens (Table 4), is $\sigma_{bc} = 457.6$ MPa. To consider the stress concentration caused by the notch (diameter change on the shaft), the fatigue limit has to be modified according to equation (15):

$$\sigma_{bc}^{*} = \frac{\sigma_{bc} \cdot \upsilon_{\sigma} \cdot \varepsilon_{s}}{\beta_{\sigma}} = \frac{457.6 \cdot 0.64 \cdot 0.8}{1.7} = 137.8 \text{ MPa} \tag{15}$$

where σ_{bc} * is the modified fatigue limit, υ_{σ} is the size factor (for the alloyed steel specimen with a diameter of 100 mm, its value is 0.64 [15]), ε_{s} is the surface factor (for a roughness of Ra = 3.2 μm, its value is 0.8 [15]) and β_{σ} is the notch concentration factor (for the given geometry and UTS, its value is 1.7 [16]).

Bending loading amplitude in the point 4:

$$\sigma_{ba} = \sigma_{b4} = 95 \text{ MPa} \tag{16}$$

To fulfil the safety requirements, the value of dynamic safety factor (17) must be higher than 1.3 ($k_{\sigma} \geq k_{min}$=1.3 [17]).

$$k_{\sigma 4} = \frac{\sigma_A}{\sigma_a} = \frac{\sigma_{bc}^{*}}{\sigma_{b4}} = \frac{137.8}{95} = 1.45 \rangle k_{\min} = 1.3 \quad \Rightarrow \text{ accomplished} \tag{17}$$

Torque loading (point 4)

Fatigue limit for the torque loading of 50CrMo4 steel evaluated for $N = 10^7$ cycles is

$$\tau_{tc} = 0.57 \cdot \sigma_{bc} = 0.57 \cdot 457.6 = 260.8 \text{ MPa} \tag{18}$$

However, this value is obtained from the fatigue limit determined by fatigue tests carried out at $R = -1$ and the torque loading is considered as $R = 0$. This means that the safety verification according to Eq. 21 must be done using a coefficient of the material sensitivity to the loading cycle asymmetry ψ_τ, which covers a potential difference in the fatigue limits obtained at different cycle asymmetry ratios.

Fatigue limit for torque loading when the notch is considered:

$$\tau_{tc}^* = \frac{\tau_{tc} \cdot \upsilon_\tau \cdot \varepsilon_s}{\beta_\tau} = \frac{260.8 \cdot 0.72 \cdot 0.8}{1.55} = 96.9 \text{ MPa} \tag{19}$$

where τ_{tc}^* is the modified fatigue limit, υ_τ is the size factor (for the alloyed steel specimen with a diameter of 100 mm, its value is 0.72 [15]), ε_s is the surface factor (for the roughness Ra = 3.2 μm, its value is 0.8 [15]) and β_σ is the notch concentration factor (for the given geometry and UTS, its value is 1.55 [16]).

Torque loading amplitude in the point 4 is expressed as:

$$\tau_{ta} = \frac{\tau_{t4}}{2} = \frac{36}{2} = 18 \text{ MPa} \tag{20}$$

where τ_{t4} is the maximal shear stress in the point 4 (Table 5).

Again, in order to fulfill the safety requirements, the value of dynamic safety factor (21) must be higher than 1.3 ($k_\tau \geq k_{min}$=1.3 [17]).

$$\begin{aligned} k_{\tau 4} &= \frac{\tau_A}{\tau_a} = \frac{\tau_{kc}^* - \psi_\tau \cdot \tau_m}{\tau_{ka}} = \frac{96.9 - 0.05 \cdot 18}{18} = 5.33 \\ k_{\tau 4} &= 5.33 \rangle k_{\min} = 1.3 \Rightarrow \text{ accomplished} \end{aligned} \tag{21}$$

where τ_m is the mean shear stress, ψ_τ is the factor representing the material sensitivity to the loading cycle asymmetry (for shear stress and UTS, it is ψ_τ = 0.05 [17]).

The total safety coefficient under the action of shear and normal stresses (point 4) (22):

$$k_{red} = \frac{k_\sigma \cdot k_\tau}{\sqrt{k_\sigma^2 + k_\tau^2}} = \frac{1.45 \cdot 5.33}{\sqrt{1.45^2 + 5.33^2}} = 1.4 \rangle k_{\min} = 1.3 \Rightarrow \text{ accomplished} \tag{22}$$

where k_σ represents the dynamic safety factor for normal stress and k_τ represents the dynamic safety factor for tangential stress.

The results given in Table 6 show that the points 4 and 6 fulfil the condition for dynamic safety k_{red} for $N = 10^7$ cycles, but not for $N = 10^9$ cycles. To satisfy the condition of dynamic safety for the shaft, it is necessary to make adjustments in the shaft design. In the point 2, the diameter size should be increased from 95 mm to 110 mm as well as the notch radius from 4 mm to 6 mm to decrease the notch concentration effect (Fig. 8). In the point 4, the shaft diameters should be increased and also the size of the splining according to Fig. 9.

Table 6 Results of loading stress and the safety coefficients for points 2 and 4 of the shaft when fatigue strengths for $N = 10^7$ cycles and $N = 10^9$ cycles are considered

Number of cycles N_f	Point i	Bending				Torque				Safety coefficient	Safety condition	Shaft weight
		σ_c /MPa	σ_{oc}* /MPa	σ_o /MPa	k_σ	τ_{kc} /MPa	τ_{kc}* /MPa	τ_{ka} /MPa	k_τ	$k_{red} = \frac{k_\sigma \cdot k_\tau}{\sqrt{k_\sigma^2 + k_\tau^2}}$	$k_\sigma, k_\tau, k_{red}$ $\geq k_{min}$=1,3	m /kg
10^7	4	457.6	137.8	95.1	1.45	260.8	96.9	18	5.3	1.4	accomplished	49.55
10^9		306	92.16	95.1	0.97	174.4	64.8	18	3.55	0.94	failed	49.55
10^7	2	457.6	132.2	100.1	1.32	-	-	-	-	-	accomplished	49.55
10^9		306	88.4	100.1	0.88	-	-	-	-	-	failed	49.55

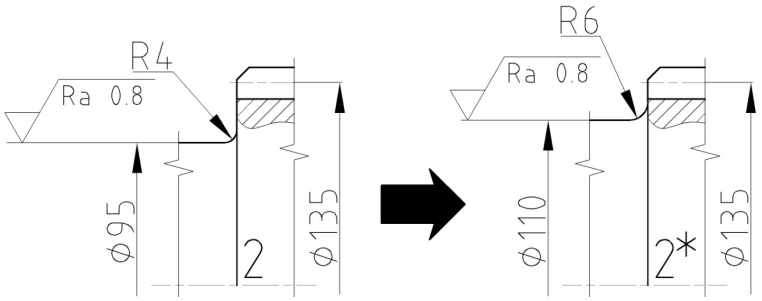

Fig.8 Adjustments in the shaft design in point 2

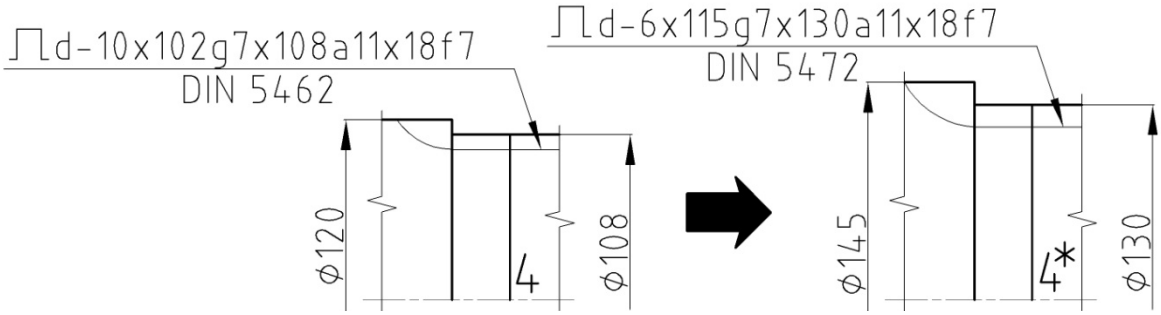

Fig. 9 Adjustments in the shaft design in point 4

After adjustments in the shaft design have been made, it is necessary to verify the shaft dynamic safety once again. The verified points of the shaft after the design adjustments are marked as 2* and 4* and the results are given in Table 7 together with a comparison with the results of the points 2 and 4 (before design adjustment). After the dimensional changes, the shaft fulfils the condition for dynamic safety for $N = 10^9$ cycles.

Table 7 Results of loading stress and the safety coefficients after design adjustments for points 2* and 4* compared to the ones calculated for points 2 and 4 (before adjustments)

Number of cycles N_f	Point i	Bending				Torque				Safety coefficient	Safety condition	Shaft weight
		σ_c /MPa	σ_{oc}* /MPa	σ_o /MPa	k_σ	τ_{kc} /MPa	τ_{kc}* /MPa	τ_{ka} /MPa	k_τ	$k_{red} = \frac{k_\sigma \cdot k_\tau}{\sqrt{k_\sigma^2 + k_\tau^2}}$	$k_\sigma, k_\tau, k_{red}$ $\geq k_{min}$=1.3	m /kg
10^9	4	306	92.16	95.1	0.97	174.4	64.8	18	3.55	0.94	failed	49.55
10^9	4*	306	89.3	63.01	1.42	174.4	63	12.2	5.11	1.37	accomplished	54.7
10^9	2	306	88.4	100.1	0.88	-	-	-	-	-	failed	49.55
10^9	2*	306	87.5	64.5	1.35	-	-	-	-	-	accomplished	54.7

4. Discussion

In the engineering practice of mechanical component design the fatigue limit obtained for $N = 10^7$ cycles is still often considered as the loading stress amplitude which provides an infinite fatigue life to the component. However, this approach cannot be adopted generally for all materials and the materials with high strength show a continuous decrease in the fatigue strength with respect to higher number of cycles [18]. This was also the case with the 50CrMo4 structural steel, where the ultrasonic fatigue tests ($f \approx 20$ kHz, $T = 20 \pm 5$ °C, $R = -1$) showed a decrease in fatigue strength from $\sigma_a = 457.6$ MPa for $N = 10^7$ cycles to $\sigma_a = 306.1$ MPa for $N = 10^9$ cycles. This represents a considerable difference in the fatigue strength of $\Delta\sigma_a = 151.5$ MPa. It can be noted that this data was obtained at high frequency testing conditions, but it has been claimed that, due to the low displacement amplitude, the deformation rate does not differ significantly from conventional tests and the influence of the high frequency is negligible [5].

According to the described conventional mechanical design of a cyclically loaded component, it is obvious that if a component is designed for the fatigue strength evaluated for $N = 10^7$ cycles it does not fulfil the safety and reliability requirements for higher numbers of cycles. The difference in fatigue strength for different numbers of loading cycles is not often covered by the safety coefficient and it is necessary to increase the component size and change the geometry of various structural notches to ensure the safe operation of the component. In this particular example, the weight of the shaft was increased by about 10 % (from 49.55 kg to 54.7 kg).

5. Conclusions

According to fatigue tests performed on 50CrMo4 structural steel in the high and the ultra-high cycle region and to the example of shaft structural design for the fatigue strength evaluated at $N = 10^7$ and $N = 10^9$ cycles, the following can be stated:

- the S – N curve of 50CrMo4 steel does not have a flat character after $N = 10^7$ cycles and the fatigue strength continuously decreases with the increasing number of cycles,
- the decrease in the fatigue strength in the range from $N = 10^7$ to $N = 10^9$ cycles is $\Delta\sigma_a = 151.5$ MPa,
- the example of cyclically loaded shaft in a gearbox with respect to the dynamic safety coefficient $k_{red} = 1.3$ shows a considerable difference in the shaft dimensions when $N = 10^7$ or $N = 10^9$ cycles are considered in the design,
- the design of the shaft for $N = 10^9$ cycles causes an increase in the shaft weight by about 10 % when compared to the design for $N = 10^7$ cycles.

Acknowledgement

The research was supported by the following institutions with projects:

- European Regional Development Fund and the Slovak State Budget for the project "Research Centre of University of Žilina", **ITMS 26220220183** (50 %).
- Slovak Research and Development Agency under the contract no. **APVV-0419-11** - Adaptation of modern computer-simulation methods to the development of rolling bearings and their verification in real conditions (25 %).
- Scientific Grant Agency of the Ministry of Education, Science, Research and Sport of the Slovak Republic under the contract no. **V-1/0396/14** (25 %).

REFERENCES

[1] Y. Murakami, Metal Fatigue: *Effects of Small Defects and Nonmetallic Inclusions*. first ed., Elsevier Oxford, 2002.

[2] S.E. Stanzl-Tschegg: *Fatigue Fract.* Eng. Mater. Struct., 22(7), 1999, pp. 567–579.

[3] C. Bathias: *There Is No Infinite Fatigue Life in Metallic Materials*. Fatigue Fract. Eng. Mater. Struct., 22(7), 1999, pp. 559–565.

[4] R.O. Ritchie, D.L. Davidson, B. L Boyce, J.P. Campbell, 0. Roder, High-Cycle Fatigue of Ti-6A1-4V, Fatigue Fract. Eng. Mater. Struct., 22(7), 1999, pp. 621–631.

[5] O. Bokůvka et al., Low and High Frequency Fatigue Testing. EDIS ŽU Žilina, 2000.

[6] Nicholas, T. 2006: *High Cycle Fatigue: A Mechanics of Materials Perspective.* 1. vyd. Oxford: Elsevier, 2006.

[7] Puškár, A. 1997. *Vysokofrekvenčná únava materiálov (High frequency fatigue of materials)*. EDIS ŽU Žilina, 1997.

[8] J. Kohout, S. Věchet: *A new function for fatigue curves characterization and its multiple merits*. International Journal of Fatigue, 23 (2001), pp.175-183.

[9] Nový, F. – Trško, L. – Bokůvka, O.: *Dynamic strength and fatigue lifetime : exercises instructions*. EDIS ŽU Žilina, 2013.

[10] Skočovský, P. et al. 2006: *Náuka o materiáli pre odbory strojnícke (Material science for students of mechanical engineering).* EDIS ŽU Žilina, 2006 (in Slovak).

[11] Bolek, A. et al..: *Časti strojů 1. svazek (Machine parts 1. volume)*. SNTL Praha, 1989 (in Czech).

[12] Bolek, A. et al.: *Časti strojů 2. svazek (Machine parts 2. volume)*. SNTL Praha, 1990 (in Czech).

[13] Várkolyová, B., Dekýš, V., Toth, Ľ.: *Pružnosť a pevnosť I (Advanced strength and applied elasticity I).* VTS pri ŽU v Žiline, 2006 (in Slovak).

[14] Kohár, R et al.: *Aplikácia optimalizačných algoritmov v mechanike telies (Application of optimization algorithms in the mechanics of bodies)*. VTS Žilina, 2006 (in Slovak).

[15] Leinveber, J., Vávra, P.: *Strojnické tabulky (Handbook of mechanical engineering)*. ALBRA, Úvaly, 2006 (in Czech).

[16] Filo, M. et al.: *Časti a mechanizmy strojov, príklady (Parts and machine mechanisms, examples).* ALFA Bratislava, 1990 (in Slovak).

[17] Málik, L. et al.: *Časti a mechanizmy strojov (Parts and machine mechanisms).* EDIS ŽU Žilina, 2003 (in Slovak).

[18] Nový, F. – Bokůvka, O. – Mintách, R. – Trško, L.: *Influence of steels strength on the ultra-high cycle fatigue lifetime*, In: Perner′s Contacts Vol. VI, No. 2, May 2011, pp. 131-135.

Submitted: 02.4.2014

Accepted: 10.12.2014

Ing. Lukáš Faturík, PhD.
doc. Ing. Slavomír Hrček PhD.
Department of Design and Mechanical Elements, Faculty of Mechanical Engineering, University of Žilina, Univerzitná 8215/1,
010 26 Žilina, Slovak Republic.
Ing. Libor Trško, PhD.
Research Centre of University of Žilina, Univerzitná 8215/1,
010 26 Žilina, Slovak Republic.
prof. Ing. Otakar Bokůvka, PhD.
Department of Materials Engineering, Faculty of Mechanical Engineering, University of Žilina, Univerzitná 8215/1,
010 26 Žilina, Slovak Republic.